

## Sporadic feedback control of flow turbulence

Guoning Tang<sup>1,2</sup> and Gang Hu<sup>1,3,4,\*</sup>

<sup>1</sup>*Department of Physics, Beijing Normal University, Beijing 100875, China*

<sup>2</sup>*College of Physics and Information Technology, Guangxi Normal University, Guilin 541004, China*

<sup>3</sup>*Chinese Center for Advanced Science and Technology (World Laboratory), Beijing 8730, China*

<sup>4</sup>*Beijing-Hong Kong-Singapore Joint Center of Nonlinear & Complex Systems (Beijing),*

*Beijing Normal University, Beijing 100875, China*

(Received 18 November 2005; revised manuscript received 27 February 2006; published 19 May 2006)

In this work we consider the problem of flow turbulence control in a two-dimensional Navier-Stokes equation. We suggest a control strategy which sporadically applies global feedback to a single velocity component of the velocity field. It is found that this control strategy can significantly enhance the control efficiency when the optimal fraction for the control period is suitably chosen, both larger and smaller control time fractions may reduce the control precision. The physical mechanism underlying this interesting and strange behavior is heuristically analyzed, based on mode-mode interactions.

DOI: [10.1103/PhysRevE.73.056307](https://doi.org/10.1103/PhysRevE.73.056307)

PACS number(s): 47.27.Rc, 05.45.Gg, 05.45.Xt

### I. INTRODUCTION

Spatiotemporal chaos (STC) can appear in a large variety of systems such as hydrodynamics, plasma devices, laser systems, chemical reactions, Josephson junction arrays, and biological networks. Because of the potential applications, controlling STC in these systems has attracted much attention of scientists and technologists in the past decade [1–11]. Real-world flow turbulence is one of the most complicated states of spatiotemporal chaos. Flow turbulence is undesirable in many cases, and control of such turbulence is thus of great interest and importance. Although many passive and active control methods have been proposed from the engineering perspectives over the last few decades [12–18], the basic dynamical methods of chaos control have been very rarely applied to the control of flow turbulence in Navier-Stokes systems.

Recently, some authors used global and local feedback control methods developed in STC control to control flow turbulence in incompressible Navier-Stokes equations (NSE) [19,20]. In Ref. [20] the authors found that by applying pinning control only to a single component (either  $u$  or  $v$  component) of the flow velocity field, the whole velocity field ( $u, v$ ) can be partially controlled to the ordered targets, in the sense that the control error is bounded by a small but non-zero constant. The main purpose of this paper is to study how to enhance the efficiency of flow turbulence control. We find that a sporadic global feedback control method can considerably improve the control results when the fraction of control time is properly chosen.

Sporadic control is known as a chaos control method that saves the control time and energy. It has been generally accepted that with the sporadic control strategy a larger fraction of control period (more control time and control energy) may achieve better control results. However, in our work we find interestingly that there exists an optimal fraction (less than 1) of control time, for the best control results, and this

optimal part-time control may achieve results better than that of the full-time control. This strange and interesting feature can be intuitively understood, based on mode-mode interactions of the turbulent system.

This paper is organized as follows. In Sec. II, the dynamical model, the numerical scheme, and the feedback control method are introduced. Section III is devoted to the description of controlling flow turbulence with sporadic feedback and demonstrating the results of this control method. The physical mechanism underlying the efficiency of the optimal sporadic control is analyzed in Sec. IV. A brief conclusion is presented in the last section.

### II. MODEL AND NUMERICAL METHOD

In this paper we consider flow turbulence described by the following incompressible two-dimensional NSE:

$$\frac{\partial \mathbf{u}}{\partial t} + \mathbf{u} \cdot \nabla \mathbf{u} = -\nabla p + \frac{1}{\text{Re}} \nabla^2 \mathbf{u}, \quad (1a)$$

$$\nabla \cdot \mathbf{u} = 0, \quad (1b)$$

with  $\mathbf{u}=(u, v)$ ,  $\mathbf{r}=(x, y)$ . Here  $p$  is the pressure, and  $\text{Re}$  the Reynolds number. Throughout this paper we keep  $\text{Re}=5000$ , and the flow is thus in the regime of fully developed turbulence. The flow is confined in a square domain  $[0, 2\pi] \times [0, 2\pi]$  with periodic boundary conditions for both  $x$  and  $y$  directions. For the numerical treatment, a Fourier pseudospectral method, the Adams-Bashforth-Crank-Nicolson scheme [21], and a dealiasing technique [22] are used together in our simulations. Spatial discretization of a  $256 \times 256$  grid is performed for the  $2\pi \times 2\pi$  physical domain. The validity of numerical results is confirmed by varying space and time steps. For freely decaying two-dimensional flow turbulence, initial conditions are important for the flow dynamics. Usually, the initial conditions are assigned in Fourier space with a specific energy spectrum such as

\*Corresponding author. Email address: ganghu@bnu.edu.cn

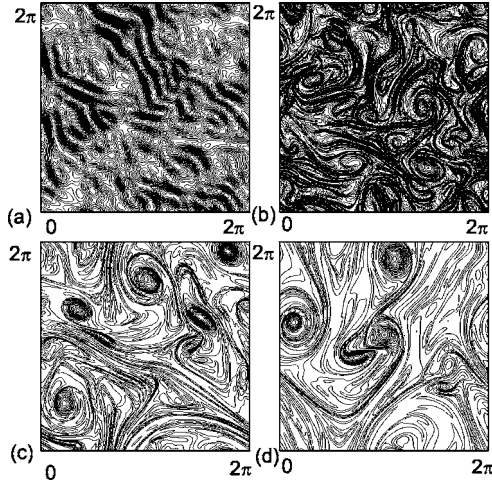


FIG. 1. Dynamic behavior of system (1) without control. The plots are contours of the vorticity field at (a)  $t=0$ , (b)  $t=5$ , (c)  $t=30$ , and (d)  $t=50$ . In the following the control signals will be applied to the state (b) for turbulence suppression.

$$E(q,0) \sim qe^{-(q/q_0)^2}, \quad (2)$$

where  $q$  is the wave number and  $q_0$  a constant. In this presentation, we use the initial energy spectrum Eq. (2) with  $q_0=5.0$ . The initial energy is 0.1. The time increment is set to  $\Delta t=0.0025$ . The total integration length is  $T=50$ , which covers several hundreds of initial eddy turnover time. In Fig. 1, we present several snapshots of turbulence evolution from  $t=0$  to 50. Some typical characteristics of two-dimensional flow turbulence, such as vortex forming, vortex collision and merging, and vortex diffusion are clearly seen. We use this turbulent dynamics as the reference for control.

Now we show how the turbulent dynamics of Fig. 1 can be controlled to a periodic target by feeding back one velocity component  $u$  only. This is motivated by the fact that in experiments, controlling a single component of velocity field could be easier than controlling the whole velocity vector. We apply the feedback control signal

$$-\varepsilon(u - u_T) \quad (3)$$

to the right-hand side of Eq. (1a), where  $u_T$  is the  $x$  component of the velocity field of the target, and  $\varepsilon$  ( $\varepsilon > 0$ ) is the control strength. In the present work, we use solutions of the NSE [21], which are spatially periodic and temporally varying, as the target for the control

$$\begin{aligned} u_T &= -\cos(qx)\sin(qy)e^{-2q^2t/\text{Re}}, \\ v_T &= \sin(qx)\cos(qy)e^{-2q^2t/\text{Re}}, \\ q &= 1, 2, 3, \dots \end{aligned} \quad (4)$$

The control is applied to the turbulent state Fig. 1(b), after the system has evolved from the initial state of Fig. 1(a) for  $t=5$ , and the evolution has passed the transient stage and reached the turbulent regime. In order to characterize the control efficiency, we define a quantity of control error between the system field and the target field at same time as

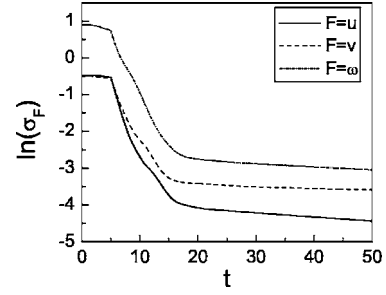


FIG. 2. Control error Eq. (5) vs time for the velocity and the vorticity when full-time control Eq. (3) with  $\varepsilon=1.0$  is applied. The target of Eq. (4) with wave number  $q=1$  is applied.

$$\sigma_F(t) = \langle [\Delta F(x,y,t)]^2 \rangle^{1/2} = \left\{ \frac{1}{(256)^2} \sum_{i=1,j=1}^{256} [\Delta F(i,j,t)]^2 \right\}^{1/2}, \quad (5)$$

where  $\Delta F(x,y,t) = F(x,y,t) - F_T(x,y,t)$ ,  $i, j$  represent the grid indices, and  $F$  may indicate a velocity component of the flow or the vorticity defined as  $\omega = v_x - u_y$ .

In Fig. 2, we present the control results of the global feedback Eq. (3) with the target Eq. (4) with  $q=1$ . It is observed that the global control method can successfully suppress flow turbulence, i.e., the control errors of the velocity components and the vorticity decay to small but nonzero constants in the given time interval  $T=50$ . Nevertheless, this nonzero value shows a certain imperfectness of control. In the next section we will show that these control errors can be considerably reduced (i.e., the control result is considerably improved) by applying sporadic control.

### III. CONTROLLING FLOW TURBULENCE WITH SPORADIC FEEDBACK SIGNAL

The central task of the present paper is to improve the precision of flow turbulence control. Namely, we focus on how to decrease the nonzero control error for a given control time length  $T$ . Intuitively, one may expect that increasing the energy of the driving signals may achieve better control results. Here we are interested in something different, namely, in improving our control effect without increasing the input energy, and with smaller total control energy. Therefore we will keep the global feedback control idea with the control strength  $\varepsilon$  unchanged, and try to achieve a better control result by changing the way feedback signals are injected.

Here we propose a control strategy of sporadic feedback. The idea of sporadic feedback is the following. The feedback control signal functions for sporadic times  $k\tau \leq t \leq (k+\gamma)\tau$  and ceases to work otherwise (see Fig. 3). With sporadic feedback control Eq. (1a) is modified to

$$\frac{\partial u}{\partial t} + u \frac{\partial u}{\partial x} + v \frac{\partial u}{\partial y} = -\frac{\partial p}{\partial x} + \frac{1}{\text{Re}} \left( \frac{\partial^2 u}{\partial x^2} + \frac{\partial^2 u}{\partial y^2} \right) - \varepsilon(t)(u - u_T), \quad (6a)$$

$$\frac{\partial v}{\partial t} + u \frac{\partial v}{\partial x} + v \frac{\partial v}{\partial y} = -\frac{\partial p}{\partial y} + \frac{1}{\text{Re}} \left( \frac{\partial^2 v}{\partial x^2} + \frac{\partial^2 v}{\partial y^2} \right), \quad (6b)$$

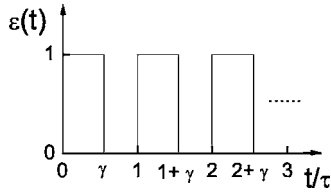


FIG. 3. Schematic figure of the sporadic control of Eq. (6c). The instant control strength  $\varepsilon(t)$  varies between 1 and 0, and the fraction of control time is  $\gamma$ .

$$\varepsilon(t) = \begin{cases} \varepsilon & \text{for } k\tau \leq t \leq (k + \gamma)\tau, \\ 0 & \text{otherwise,} \end{cases} \quad (6c)$$

$$0 \leq \gamma \leq 1, \quad k = 0, 1, 2, \dots$$

The ratio  $\gamma$  is the fraction of time period when control is applied. We find that there exists an optimal fraction  $\gamma < 1$  at which the control reaches the best efficiency (the smallest control error  $\sigma_F$ ), considerably better than that of full-time control of  $\gamma = 1$ .

In Fig. 4(a), we do the same as in Fig. 2 with sporadic feedback using  $\tau = 0.5$  and  $\gamma = 0.55$ . It is observed that sporadic control can suppress flow turbulence faster than full-time feedback control of Fig. 2, and the control errors decay to values smaller than those of full-time control for the same evolution time period ( $T = 50$ ). In Fig. 4(b) we plot the contour figure of the vorticity field after the sporadic control of Eq. (6c) is applied to the turbulent state Fig. 1(b) for  $t = T = 50$ . The ordered target is perfectly realized and the turbulent state of Fig. 1(d) is satisfactorily suppressed. In order to have a quantitative comparison between various sporadic controls for different  $\gamma$  and  $\tau$ , we plot in Fig. 5(a)  $\sigma_\omega(50)$  vs  $\gamma$  for  $\tau = 0.25$  (black squares) and  $\tau = 0.5$  (circles), respectively. We find an optimal ratio about  $\gamma = 0.55$ , at which sporadic control can reach minimum vorticity control error, which is about eight times smaller than that for the full-time feedback control. In Figs. 5(b)–5(d) we plot the contours of  $\Delta\omega(x, y, t = 50)$ ,

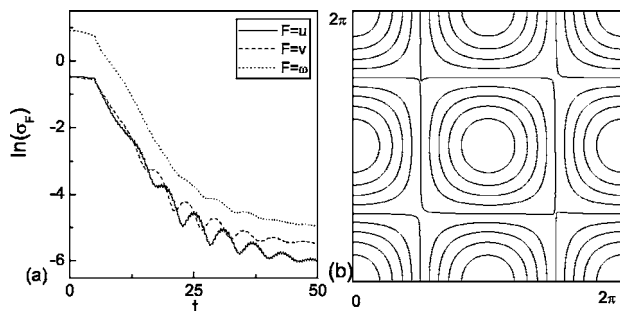


FIG. 4. (a) The same as Fig. 2 with sporadic control of  $\tau = 0.5$  and  $\gamma = 0.55$  applied. The control errors are considerably reduced with the part-time control of  $\gamma \approx 0.55$  in comparison with the full-time control of Fig. 2. (b) Contour plot of the vorticity field of the system at  $t = 50$ . The target is reached perfectly with the application of sporadic control of 55% control time.

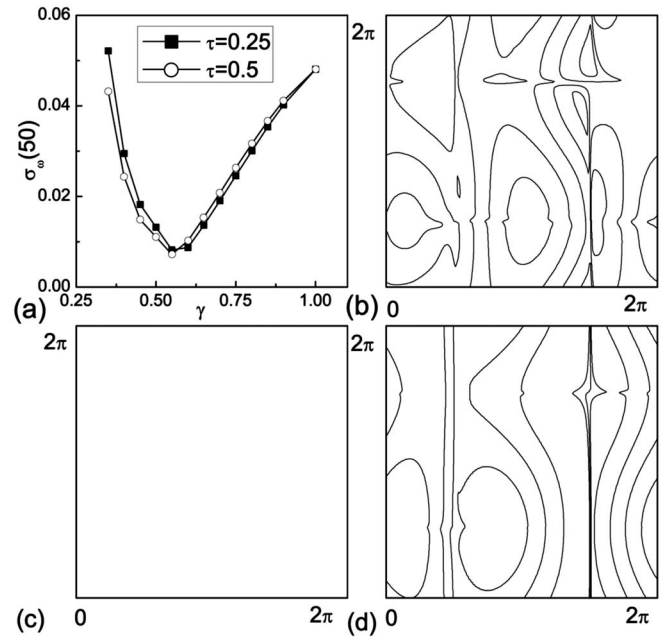


FIG. 5. (a) Control errors defined in Eq. (5) vs the fraction of control time  $\gamma$ . The control strength and the target state are the same as Fig. 2. There exists an optimal fraction  $\gamma \approx 0.55$ , at which the control can reach much higher (about eight times higher) control precision than the full-time control of  $\gamma = 1$ . (b)–(d) The contour plots of vorticity error defined in Eq. (7) for  $\tau = 0.5$  and different  $\gamma$ 's. (b)  $\gamma = 0.35$ . (c)  $\gamma = 0.55$ . (d)  $\gamma = 1.0$ . The scale of the three contour plots are identical.

$$\Delta\omega(x, y) = \omega(x, y) - \omega_T(x, y), \quad (7)$$

for different  $\gamma$ . It is clear that with the same scale measuring the control errors,  $\Delta\omega$  for the optimal  $\gamma$  ( $\gamma \approx 0.55$ ) is not directly viewable while these errors can be observed clearly for both larger ( $\gamma = 1.0$ ) and smaller ( $\gamma = 0.35$ )  $\gamma$ 's.

The behavior shown in Figs. 4 and 5 is interesting as well as surprising. In chaos control we are familiar with various sporadic control methods which are usually applied for the sake of saving control energy or better masking the messages of transmitted signals [23–25]. Nevertheless, it is generally accepted that sporadic control with a larger fraction of control time [i.e., larger  $\gamma$  in Eq. (6c)] can reach better control results than with a smaller fraction of control time, because longer time injection can inject larger control energy, and this is favorable to the suppression of turbulence. In this regard, the effect of full-time control ( $\gamma = 1$ ) is expected to be always better than that of part-time sporadic control ( $1 > \gamma > 0$ ). In Fig. 5(a) we find that  $\sigma_\omega(50)$  decreases (i.e., the control precision increases) as  $\gamma$  decreases (the control time decreases) from  $\gamma = 1$ , and this is strongly against the above intuition. We will explain heuristically this anti-intuition phenomenon in the next section.

#### IV. MECHANISM UNDERLYING THE HIGH EFFICIENCY OF OPTIMAL SPORADIC TURBULENCE CONTROL

The results in Fig. 5 can be heuristically understood, based on mode-mode interactions. We make the Fourier transformation of  $u$  and  $v$  as

$$\begin{aligned}
 F(x, y, t) = & \sum_{m=0, n=0}^{\infty} [A_{Fa}(m, n, t)\cos(mx)\cos(ny) \\
 & + A_{Fb}(m, n, t)\sin(mx)\cos(ny) \\
 & + A_{Fc}(m, n, t)\cos(mx)\sin(ny) \\
 & + A_{Fd}(m, n, t)\sin(mx)\sin(ny)], \\
 F = & u, v, p, \tag{8}
 \end{aligned}$$

where  $A(m, n, t)$  is the amplitude of a mode  $(m, n)$ . There are four types of modes (a, b, c, d) for a single wave number  $(m, n)$ . By using the incompressibility condition Eq. (1b), we obtain

$$mA_{ua}(m, n, t) = nA_{vd}(m, n, t), \quad mA_{ub}(m, n, t) = -nA_{vc}(m, n, t), \tag{9a}$$

$$mA_{uc}(m, n, t) = -nA_{vb}(m, n, t), \quad mA_{ud}(m, n, t) = nA_{va}(m, n, t), \tag{9b}$$

$$A_{ua}(m, 0, t) = A_{va}(0, n, t) = 0, \quad A_{ub}(m, 0, t) = A_{vc}(0, n, t) = 0, \tag{9c}$$

$$A_{ua}(0, n, t) \neq A_{va}(m, 0, t), \quad A_{uc}(0, n, t) \neq A_{vb}(m, 0, t), \tag{9d}$$

$$n, m \neq 0.$$

The reason why the two components of the velocity field of NSE can be controlled to the periodic target by applying feedback injections to a single component only can be explained through mode-mode interactions. In order to understand the control mechanism, we transform the controlled NSE (6) to the mode amplitude form as

$$\begin{aligned}
 \frac{\partial A_u(m, n, t)}{\partial t} = & \varepsilon[A_T(m, n, t) - A_u(m, n, t)] - \frac{1}{\text{Re}}(m^2 + n^2) \\
 & \times A_u(m, n, t) - p_u(m, n, t) + [\delta_{inu}(m, n, t) \\
 & - \delta_{ouu}(m, n, t)A_u(m, n, t)], \tag{10a}
 \end{aligned}$$

$$\begin{aligned}
 \frac{\partial A_v(m, n, t)}{\partial t} = & -\frac{1}{\text{Re}}(m^2 + n^2)A_v(m, n, t) - p_v(m, n, t) \\
 & + [\delta_{inv}(m, n, t) - \delta_{out}(m, n, t)A_v(m, n, t)]. \tag{10b}
 \end{aligned}$$

The last terms of the right-hand sides of Eq. (10)  $\delta_{in}(m, n, t)$  and  $\delta_{out}(m, n, t)A(m, n, t)$  have rather complicated forms related to mode-mode interactions such as

$$u \frac{\partial u}{\partial x} + v \frac{\partial u}{\partial y}, \quad u \frac{\partial v}{\partial x} + v \frac{\partial v}{\partial y}. \tag{11}$$

Instead of specifying their complicated forms, we simply remark that  $\delta_{in}(m, n, t)$  and  $\delta_{out}(m, n, t)A(m, n, t)$  are related to the energy gain and energy loss of mode  $(m, n)$  through mode-mode interactions, respectively, and they decrease as

the amplitudes of the interacting modes decrease. From Eq. (10) it is clear that the feedback signal is applied to the  $u$  component, and thus all modes of this component are directly controlled. On the other hand, the modes of  $v$  component appearing in Eqs. (9a)–(9c) are coupled with some of the  $u$  modes strictly through the incompressibility condition, and thus can also be regarded to be controlled by the feedback signal directly (called the direct modes). Since the feedback control has a dissipative nature, all the above modes may be driven by the control signal to zero or to the target [(1,1) mode] in a direct way. However, there exist some modes of the  $v$  component [the  $v$ -modes in Eq. (9d)] which are neither directly controlled by the feedback signal, nor strictly related to the direct modes. These modes are indirectly controlled modes (simply called the indirect modes afterwards), they are influenced by the control through the mode-mode interactions of the NSE dynamics Eq. (10), and these modes have relatively lower damping rates. In particular, the indirect modes with small wave numbers (i.e., small  $m$ ) have the most serious effects on the control errors. On the one hand, these modes damp to zero slowly, yielding large  $\sigma_v$  [i.e., large  $A_v(m, 0, t)$ ]. On the other hand, these large  $A_v(m, 0, t)$  can also influence the direct modes through mode-mode interactions [i.e., yield relatively large  $\delta_{inu}(m, n, t)$ ] and make the direct modes damp to zero slowly too. This leads also to relatively large control errors  $\sigma_u$  and  $\sigma_\omega$ .

Based on the above picture we can heuristically explain why the optimal part-time control can achieve results better than that of the full-time control. With full-time control, the direct modes may damp quickly in the early stage of the evolution, while the indirect modes hardly feel the influence of the control, so that the amplitudes of the direct modes become very small in comparison with the indirect modes. This makes the coupling from the direct modes to the indirect modes ineffective and consequently makes the damping of the indirect modes slow. The slowness of the indirect-mode damping produces the large control error  $\sigma_v$  in Fig. 2 and also a relatively large control error  $\sigma_u$  through the coupling. With the optimal sporadic feedback, the direct modes damp a bit slowly and both the direct and the indirect modes have similar damping rates. Then the amplitudes of both direct and indirect modes are comparable, and there exist relatively large interactions between both types of modes, allowing all the modes to damp more effectively than the full-time control. This effect considerably reduces the control errors in Fig. 4. This explanation is supported by the following observation: full-time control of  $\gamma=1$  is always better than any sporadic control of  $\gamma<1$  if the feedback signals are applied to both  $u$  and  $v$  components as shown in Fig. 6. (Then all modes are directly controlled by the feedback signals and mode-mode interactions are not of crucial importance for the control.)

The investigation of Sec. III was conducted for a target with wave number  $q=1$ , and a single quantity of control error  $\sigma_F$  [Eq. (5)] was used for measuring the control results. To end the present section we briefly discuss the control results for a target with high wave number by measuring the behavior of some other important physical quantities. Specifically, we use the target of Eq. (4) with  $q=3$ , and study the evolutions of energy  $E$  and enstrophy  $E_\omega$

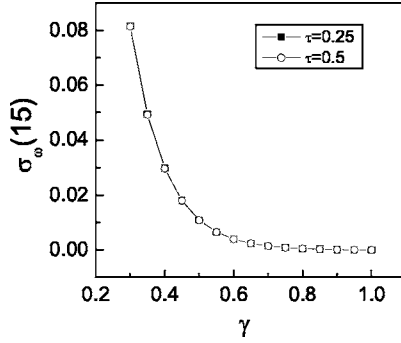


FIG. 6. The same as Fig. 5(a) with both components ( $u, v$ ) of Eq. (1) being controlled by the feedback signals  $\varepsilon(t)(u_T - u)$  and  $\varepsilon(t)(v_T - v)$ , respectively, with  $T=15$ ,  $\tau=0.25, 0.5$ . Since all modes are directly controlled by the feedback signals, mode-mode interactions are not crucial for the control efficiency. Now  $\sigma_\omega(T=15)$  is minimum at full time control  $\gamma=1$ , and  $\sigma_\omega(15)$  increases monotonically as  $\gamma$  decreases.

$$E(t) = \frac{1}{2(2\pi)^2} \int (u^2 + v^2) dx dy, \quad (12a)$$

$$E_\omega(t) = \frac{1}{2(2\pi)^2} \int \omega^2 dx dy, \quad (12b)$$

respectively.

In Fig. 7(a) we do the same as Fig. 5(a) with target  $u_T$  replaced by  $q=3$ . The optimal sporadic control can be observed at  $\gamma \approx 0.41$ . In Figs. 7(b) and 7(c) we measure the energy  $E$  and enstrophy  $E_\omega$ , respectively, for the case of free evolution (solid lines). It is found that the energy of turbulent flow damps slowly, and the enstrophy damps quickly in the early time stage and then decreases slowly at a certain non-zero level (about  $E_\omega \approx 0.26$ ). On the other hand, with control both energy and enstrophy (with the target components excluded) damp much quicker than those without control, indicating quick suppression of turbulence by control [dashed lines in Figs. 7(b) and 7(c)]. In Fig. 7(d) we plot a snapshot of the contour pattern of the vorticity field of the system under control at  $T=50$  under control. The  $q=3$  mode ordering (with some imperfection) is obviously established. In order to understand the detailed evolution and exchange of the energy of different modes, we define the energy of  $q$  mode as

$$E_q(t) = \frac{1}{2(2\pi)^2} \int (u_q^2 + v_q^2) dx dy, \quad (13)$$

$$u_q(t) = -A_u(q, t) \cos(qx) \sin(qy),$$

$$v_q(t) = A_v(q, t) \sin(qx) \cos(qy),$$

$$q = 1, 2, \dots, 10$$

and we plot variations of the energies of various  $q$  modes without [Fig. 8(a)] and with [Fig. 8(b)] control. It is observed that without control the energies of different modes oscillate randomly with time, together with a slow damping. The modes of large wave vectors have smaller energies. With

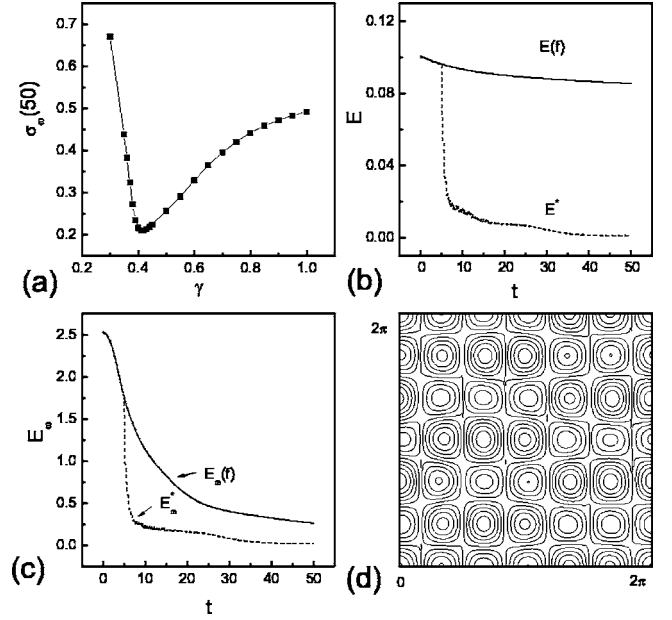


FIG. 7. Results of sporadic control with  $\tau=0.5$  and the target state  $u_{3T} = -0.5 \cos(3x) \sin(3y) e^{-2 \times 3^3 / \text{Re}}$  and  $v_{3T} = 0.5 \sin(3x) \times \cos(3y) e^{-2 \times 3^3 / \text{Re}}$ . The control strength is  $\varepsilon=3$ . (a) The same as Fig. 5(a) with the target replaced by  $q=3$ . An optimal time fraction of control  $\gamma=0.41$  is seen. (b)–(d) Part-time control with  $\gamma=0.41$  is applied. (b) Solid line:  $E(f)$  defined in Eq. (12a) without control plotted vs  $t$ . Dashed line:  $E^*$  defined by the difference of the total energy  $E$  of Eq. (12a) and the target mode energy.  $E^*$  damps much more quickly than  $E(f)$ , indicating the quick suppression of turbulence by control. (c) The same as (b) with the enstrophy  $E_\omega$  measured. (d) Contour pattern of the vorticity field of the system under control at  $t=50$ .

control the energy of the target mode increases quickly to a certain value and then remains there almost unchanged over the time interval  $t \leq T=50$ . Note that the target energy should also damp according to the rule of Eq. (4); the damping rate is, however, very small for large Reynolds number  $\text{Re} \gg 1$ . An interesting observation in Fig. 8(b) is that  $E_3$  can increase from a value much smaller than  $E_1$  and  $E_2$  to a value much larger than them, indicating an upstream energy flow by turbulence control.

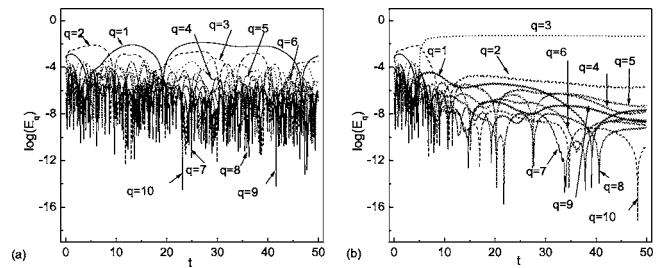


FIG. 8. Energy  $E_q$  of modes ( $q, q$ ),  $q=1, 2, \dots, 10$  plotted vs  $t$ . (a) Energies  $E_q$  plotted vs time without control. (b) Energies  $E_q$  plotted vs time with sporadic control of  $\gamma=0.41$ . The control parameters and the target state are the same as Fig. 7(d).

## V. CONCLUSION

In summary, we have studied the problem of controlling flow turbulence by applying global sporadic feedback signals to a single velocity component. We find that part-time sporadic control may obtain better control results than full-time control if the fraction of control time is properly chosen. It is a significant result to use lower energy for the control signals to achieve lower control error with the same control strength and the same evolution time length. This interesting achievement is physically understood based on mode-mode interactions during the control process.

The practical realization of dynamical control of flow turbulence turns out to be a difficult and complicated task from an engineering perspective. The control scheme used in the

present study is an active control strategy. This method requires instant variable measurement, and immediate feedback injection. Such direct flow manipulations are difficult. Nevertheless, we can expect that the realization of this control strategy may become possible with the development of new microsensors and microactuators of micron size, fabricated by microelectromechanical-systems (MEMS) technology. Our theoretical work will shed light on flow turbulence control in realistic applications.

## ACKNOWLEDGMENTS

This work was supported by the Natural Science Foundation of China (Grant No. 10335010) and National 973 project of Nonlinear Science.

- 
- [1] G. Hu and K. He, *Phys. Rev. Lett.* **71**, 3794 (1993).
  - [2] G. Hu and Z. Qu, *Phys. Rev. Lett.* **72**, 68 (1994).
  - [3] D. Auerbach, *Phys. Rev. Lett.* **72**, 1184 (1994).
  - [4] F. Qin, E. E. Wolf, and H.-C. Chang, *Phys. Rev. Lett.* **72**, 1459 (1994).
  - [5] W. Lu, D. Yu, and R. G. Harrison, *Phys. Rev. Lett.* **76**, 3316 (1996).
  - [6] K. Hu and G. Hu, *Phys. Rev. E* **53**, 2271 (1996).
  - [7] M. Z. Ding, E.-J. Ding, W. L. Ditto, B. Gluckman, V. In, J.-H. Peng, M. L. Spano, and W. M. Yang, *Chaos* **7**, 644 (1997).
  - [8] L. Kocarev, V. Parlitz, T. Stojanovski, and P. Janjic, *Phys. Rev. E* **56**, 1238 (1997).
  - [9] J. Xiao, G. Hu, J. Yang, and J. Gao, *Phys. Rev. Lett.* **81**, 5552 (1998).
  - [10] O. Beck, A. Amann, E. Schöll, J. E. S. Socolar, and W. Just, *Phys. Rev. E* **66**, 016213 (2002).
  - [11] P. Parmananda, B. J. Green, and J. L. Hudson, *Phys. Rev. E* **65**, 035202(R) (2002).
  - [12] M. Gad-el-Hak, *Flow Control* (Cambridge University Press, Cambridge, England, 2000).
  - [13] B. S. V. Patnaik and G. W. Wei, *Phys. Rev. Lett.* **88**, 054502 (2002).
  - [14] N. V. Nikitin, *Fluid Dyn.* **38**, 854 (2003).
  - [15] F. Li and N. Aubry, *Phys. Fluids* **15**, 2163 (2003).
  - [16] R. Rathnasingham and K. S. Breuer, *J. Fluid Mech.* **495**, 209 (2003).
  - [17] J. G. Pang and K.-S. Choi, *Phys. Fluids* **16**, L35 (2004).
  - [18] T. Min and J. Kim, *Phys. Fluids* **16**, L55 (2004).
  - [19] S. Guan, Y. C. Zhou, G. W. Wei, and C.-H. Lai, *Chaos* **13**, 64 (2003).
  - [20] S. Guan, G. W. Wei, and C.-H. Lai, *Phys. Rev. E* **69**, 066214 (2004).
  - [21] S. Y. Yang, Y. C. Zhou, and G. W. Wei, *Comput. Phys. Commun.* **143**, 113 (2002).
  - [22] C. Canuto, M. Y. Hussaini, A. Quarteroni, and T. A. Zang, *Spectral Methods in Fluid Dynamics* (Springer-Verlag, New York, 1987).
  - [23] L. Kovarev and U. Parlitz, *Phys. Rev. Lett.* **77**, 2206 (1996).
  - [24] T. Stojanovski, L. Kocarev, U. Parlitz, and R. Harris, *Phys. Rev. E* **55**, 4035 (1997).
  - [25] L. Junge and U. Parlitz, *Phys. Rev. E* **64**, 055204 (2001).